

On Convergence of Training Loss Without Reaching Stationary Points

Jingzhao Zhang*

Haochuan Li

Suvrit Sra

Ali Jadbabaie

jzhzhang@mit.edu

haochuan@mit.edu

suvrit@mit.edu

jadbabai@mit.edu

Abstract

It is a well-known fact that nonconvex optimization is computationally intractable in the worst case. As a result, theoretical analysis of optimization algorithms such as gradient descent often focuses on local convergence to *stationary points* where the gradient norm is zero or negligible. In this work, we examine the disconnect between the existing theoretical analysis of gradient-based algorithms and actual practice. Specifically, we provide numerical evidence that in large-scale neural network training, such as in ImageNet, ResNet, and WT103 + TransformerXL models, the Neural Network weight variables *do not* converge to stationary points where the gradient of the loss function vanishes. Remarkably, however, we observe that while weights do not converge to stationary points, the value of the loss function converges. Inspired by this observation, we propose a new perspective based on ergodic theory of dynamical systems. We prove convergence of the distribution of weight values to an approximate invariant measure (without smoothness and assumptions) that explains how the training loss can stabilize without weights necessarily converging to stationary points. We further discuss how this perspective can better align the theory with empirical observations.

1 Introduction

It would not be controversial to claim that there currently exists a wide gulf between theoretical investigations of convergence to stationary points for non-convex optimization problems of the form

$$\min_{\theta} f(\theta), \quad (1)$$

and the empirical performance of popular algorithms used in deep learning practice. Due to the intrinsic intractability of general nonconvex problems, theoretical analysis of nonconvex optimization problems is often focused on the rates of convergence of gradient norm $\|\nabla f(\theta)\|$ instead of the sub-optimality $f(\theta) - \min_{\theta} f(\theta)$. The vast theoretical literature on optimization for machine learning has documented the recent progress in this area. In particular, optimal gradient-based algorithms and rates have been identified in various nonconvex settings, including deterministic, stochastic and finite-sum problems [Carmon et al., 2017, Arjevani et al., 2019, Fang et al., 2018].

In addition to theoretical interests in such problems, a practical motivation for such convergence analyses is to improve the convergence rate of large-scale optimization methods as they are used in machine learning practice, especially in training deep neural networks. As neural network models allow for efficient gradient evaluations, gradient-based algorithms have been the dominant methods to tune network parameters. Naturally, great effort was dedicated to theoretical understandings of gradient-based optimizers.

However, despite the fast progress on the theory side for gradient-based algorithms, the convergence analysis has had a limited impact on real-world neural network training. Despite many theoretical and empirical advances, the gap between theory and practice is as wide as ever. As an example, consider the variance reduction technique. Even though variance reduction theoretically accelerates convergence, recent empirical evidence in [Defazio and Bottou, 2018] suggests that it may be ineffective in speeding up neural network training. On the other extreme, ADAM [Kingma and Ba,

*This work is done while visiting IIIS Tsinghua.

2014] is among the most popular algorithms in neural network training, yet its theoretical convergence was proven to be incorrect [Reddi et al., 2019]. Despite dubious theoretical properties, ADAM is as popular as ever.

Our goal in this work is to address a very specific part of this theory-practice divide by providing an explanation for the ineffectiveness of theoretical convergence rates to stationarity in neural network training. First, we provide evidence that in many real-world experiments (e.g. ImageNet, Wiki103) where the model does not overfit the data, gradient-based optimization methods do not converge to stationary points as theory predicts. This questions applicability of one of the key pillars of optimization theory as applied to neural network training. The reason for such a surprising divide is that most optimization analyses for deep learning either assume smoothness directly which leads to convergence to stationary points using classical analysis, or prove smoothness and fast convergence by relying explicitly on overparametrization. However, our empirical investigations reveal that the key premise of the theory—pointwise convergence to a fixed point—may not happen at all in practice.

Motivated by this observation, we aim to answer the following question in the rest of this work: *how should one define and analyze convergence of gradient-based optimization, when the training loss seems to converge yet the gradient does not converge to 0?*

We propose a new lens through which one should view convergence: rather than convergence of weights, we postulate that the convergence should be viewed in terms of invariant measures as used in the ergodic theory of dynamical systems. Using classical results from this literature, we then show how this new perspective can be consistent with some recent curious findings in neural network training, such as relaxed smoothness [Zhang et al., 2019] and edge of stability [Cohen et al., 2021, Wu et al., 2018] phenomena. More concretely, our contributions are summarized as follows,

- We empirically verify through ResNet training and transformer-XL training in a wide range of applications that the iterates do not converge to a stationary point as existing theory predicts.
- We propose the invariant measure perspective from dynamical systems theory so as to explain why the training loss can converge without the iterates converging to a stationary point.
- Most importantly, we show that our theorems on diminishing gain of the loss without vanishing of the gradient apply to neural network training even without standard global Lipschitzness or smoothness assumptions.
- We discuss how our observations relate to interesting phenomena such as decay of function values, edge of stability, and relative smoothness.

1.1 Related work

Many recent results inspired us to investigate the oscillatory behavior of neural network training. One line of work is on the empirical investigations of neural network reproducibility. In [Henderson et al., 2017], authors analyzed the stability of policy reward in reinforcement learning and found large variations. In [Madhyastha and Jain, 2019], authors studied the instability for interpretation mechanisms. In [Bhojanapalli et al., 2021], authors found that though image classification has relatively stable classification accuracy, the actual prediction on individual images has large variations. We learned from recent studies [Cohen et al., 2021, Zhang et al., 2019, 2020a] that previous analysis assumptions on noise and smoothness not only have large variations but also adapt to the step size choice. These observations motivate us to rethink the convergence proofs used in classical optimization analysis. In addition, a few very recent results reported similarly large oscillations in Cifar10 training [Li et al., 2020, Kunin et al., 2021, Lobacheva et al., 2021], though the authors focus on SDE approximation or batch normalization. Our work instead focuses on the connection to nonconvex optimization theorems. Specifically we show that at the end of training when training loss has converged, even the full batch gradient norm does not converge to zero.

On the theory side, two lines of work are closely related to this paper. One line of work studied the non-convergence of dynamics of algorithms in games or multiobjective optimization [Hsieh et al., 2019, Cheung and Piliouras, 2019, Papadimitriou and Piliouras, 2019, Letcher, 2020, Flokas et al., 2020]. Another modeled the SGD dynamics via the Langevin dynamics [Cheng et al., 2020, Li et al.,

2020, Gurbuzbalaban et al., 2021]. Our work differs from these works in that we do not look for global mixing and do not focus on settings where additional noise needs to be injected.

2 Motivating examples

In order to start our exposition, we provide some initial experimental results and show that the traditional notion of convergence for nonconvex functions does not really occur in deep neural network training. Our experiments are based on one of the most popular training schemes, where we trained ResNet101 on ImageNet¹. More experiments can be found later in Section 6.

To explain the quantities of interest, we first define our notation. Let $S = \{(x^i, y^i)\}_{i=1}^N$ be the dataset. We use $f(x, \theta)$ to denote the neural network function with model parameter θ and data input x . We use ℓ to denote the loss function such as cross-entropy after softmax. We would like to investigate the evolution of the following quantities during training. At iteration k , we evaluate

$$\begin{aligned} \text{Loss: } L_S(\theta_k) &:= \frac{1}{N} \sum_{i=1}^N \ell(f(x^i, \theta_k), y^i), \\ \text{Grad norm: } \|\nabla L_S(\theta_k)\|_2 &:= \left\| \frac{1}{N} \sum_{i=1}^N \frac{\partial}{\partial \theta} \ell(f(x^i, \theta_k), y^i) \right\|_2, \\ \text{Noise: } \sigma(\theta_k) &:= \sqrt{\frac{1}{N} \sum_{i=1}^N \left\| \nabla L_S(\theta_k) - \frac{\partial}{\partial \theta} \ell(f(x^i, \theta_k), y^i) \right\|_2^2}, \\ \text{Sharpness: } \|\nabla^2 L_S(\theta_k)\|_{\text{op}} &:= \left\| \frac{1}{N} \sum_{i=1}^N \frac{\partial^2}{\partial \theta^2} \ell(f(x^i, \theta_k), y^i) \right\|_{\text{op}}, \end{aligned} \quad (2)$$

where $\|\cdot\|_2$ is the standard vector ℓ_2 norm and $\|\cdot\|_{\text{op}}$ is the induced matrix spectral norm.

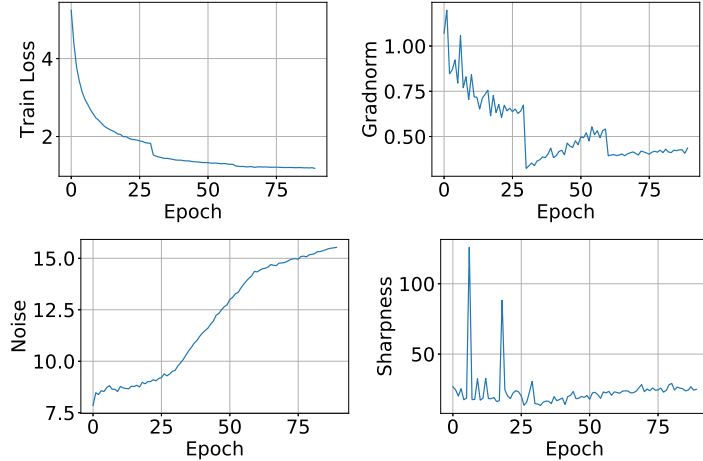


Figure 1: The quantities of interest (2) vs epoch for the default training schedule of ImageNet+ResNet101 experiment.

We then show how the trajectory of weights evolves for the standard training schedule, i.e., the learning rate starts at 0.1 and is decayed by a factor of 10 every 30 epochs. Evolution of the quantities is plotted in Figure 1. We make the following immediate observations:

- Within each period where the step size is held constant, the change in loss converges to 0.
- The gradient norm does not converge to 0 despite the fact that the loss function converges. In fact, the gradient norm is not significantly smaller than that at the start of the optimization.
- The noise level (in the stochastic gradient) increases during training.

The above observations suggest that there is *a major gap between theory and practice*. Much of the research on nonconvex optimization has focused on the convergence rate of gradient norms under

¹We used the procedure from GitHub repository <https://github.com/jiweibo/ImageNet>, and were able to reproduce the original paper's result [He et al., 2016] up to 1% validation accuracy.

a bounded-smoothness, bounded-noise setup. Faster algorithms are designed under this guidance. However, in practice, we find that the convergence of the training loss does not require the convergence of gradient norms. This may be the reason why techniques such as variance reduction or local regularization combined with Nesterov-momentum have had limited practical use, despite their massive theoretical popularity.

2.1 Different learning rates and training schedules

One immediate question following the observation in Figure 1 is whether the observed phenomenon holds solely for a particular stage-wise learning rate, which is not very common in theoretical analysis. In this subsection, we show that this cannot be the reason and that the gradient norm does not converge to zero for *any* learning rate schedule. In particular, we run the same ResNet101 model on the ImageNet dataset just as before, except that we use a constant learning rate across all 90 epochs of training. The quantities are summarized in Figure 2. A quick glance at the plots verifies that gradient norm does not converge to 0 in any of the experiments. We further notice that a smaller learning rate leads to larger gradient norm, larger stochastic gradient noise intensity, and larger sharpness as observed in [Cohen et al., 2021]. We will further discuss the implications of these observations later in the paper.

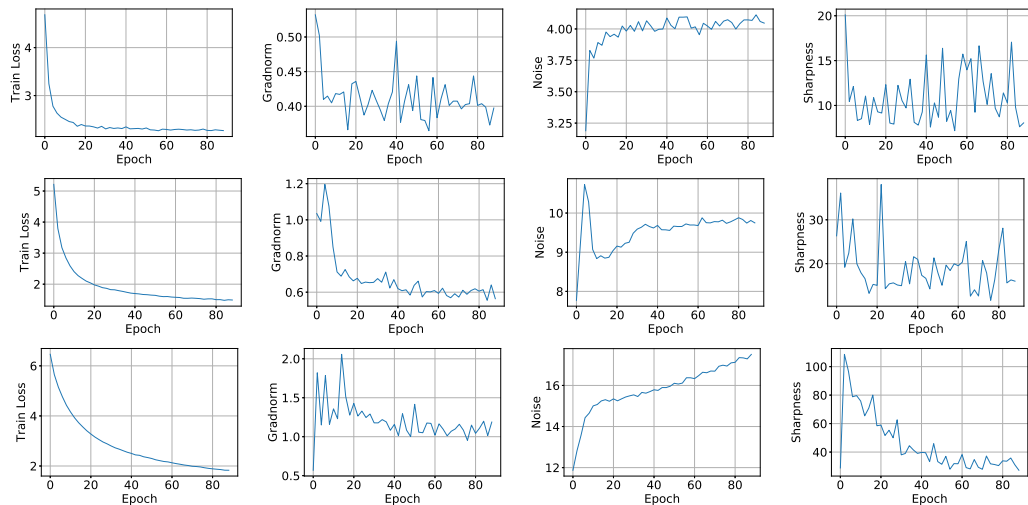


Figure 2: The quantities of interest (2) vs epoch for the constant learning rate training schedule in ImageNet experiments. The learning rate is set to be 0.1, 0.01, 0.001 from the top row downwards. All models are trained for 90 epochs.

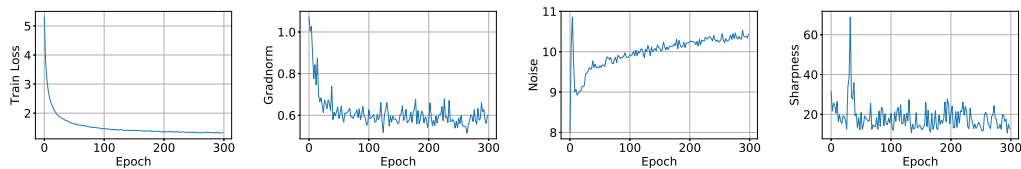


Figure 3: The estimated stats vs epoch for the constant learning rate $\eta = 0.01$ training schedule with total 300 epochs.

As the loss curves in the last two rows of Figure 2 are still decreasing, we continue the second row experiment (step size $\eta = 0.01$) for 300 epochs and present the result in Figure 3.

The above experiments show that in ImageNet+ResNet101 experiment, iterates of the weights do not converge to stationary points. In the next section, we test whether this phenomenon was an artifact of the data set and architecture and try to see if this also happens in other datasets and architectures.

2.2 Transformer XL experiments

We run Transformer-XL training on WT103 dataset for the language modeling task following the implementation of the original authors [Dai et al., 2019b]. Our training procedure is exactly the same as the official code, except that we reduce the number of attention layers for the baseline model from 6 to 4 so that the batch size fits in our GPU memory. Aside from training with a cosine learning rate schedule with initial learning rate $\eta = 0.00025$, we also experimented with different constant learning rates. The result is summarized in Figure 4.

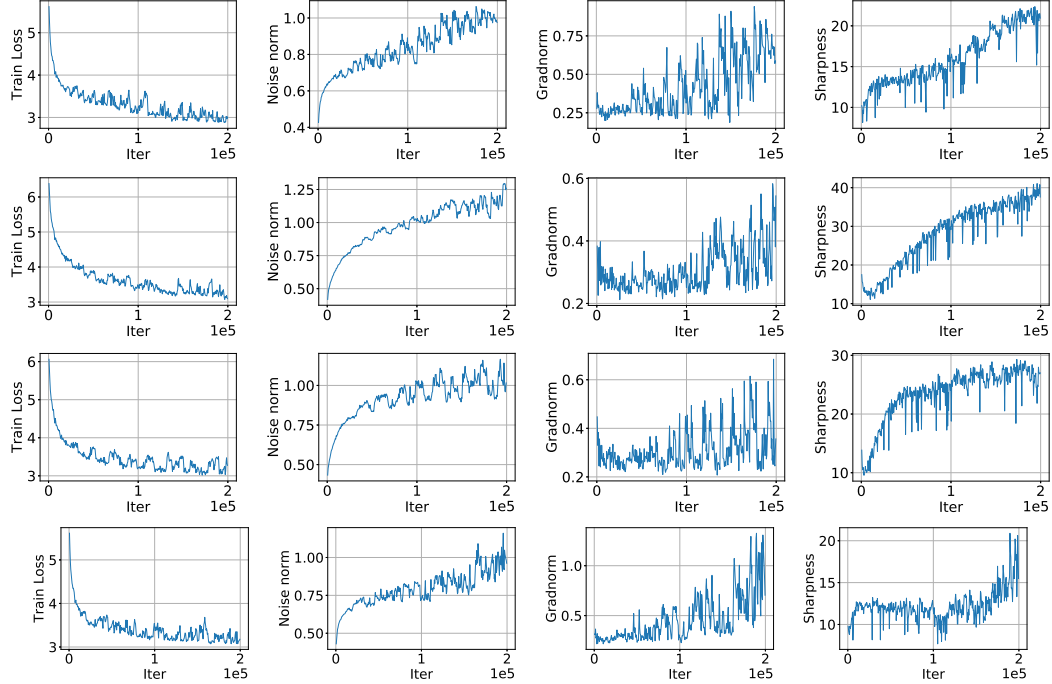


Figure 4: The estimated stats vs epoch for the transformer XL training. The learning rate is set to be cosine learning rate with $\eta = 0.00025$ in the first row. The learning rates are constant learning rates with $\eta = 0.00005, 0.0001, 0.00025$ from the second row downwards.

We found that the observations made before also apply to transformer XL training. In particular, the gradient norm is not going to 0, and even not decreasing over the training. Furthermore, smaller step size also leads to larger gradient norm.

2.3 Refuted hypotheses and potential causes

With the above experiments, we can already **exclude** some explanations on why gradient norm does not converge to zero.

1. The large gradient norm is due to the fact that the step size is not small enough or the model is not trained long enough.
2. This phenomenon is restricted to the particular ResNet + ImageNet combination.
3. The step size decreased too fast before the gradient norm could converge.
4. The large gradient norm is due to numerical or estimation error.

The first conjecture is excluded by comparing the experiment in Figure 3 against the experiments in the first two rows of Figure 2. We find that after running longer with a smaller step size, though the training loss dropped significantly, the gradient norm did not decrease at all. *This confirms that even the qualitative theoretical results (let alone the quantitative convergence rates) on when gradient norm gets smaller from canonical optimization analysis is not applicable to neural network training.*

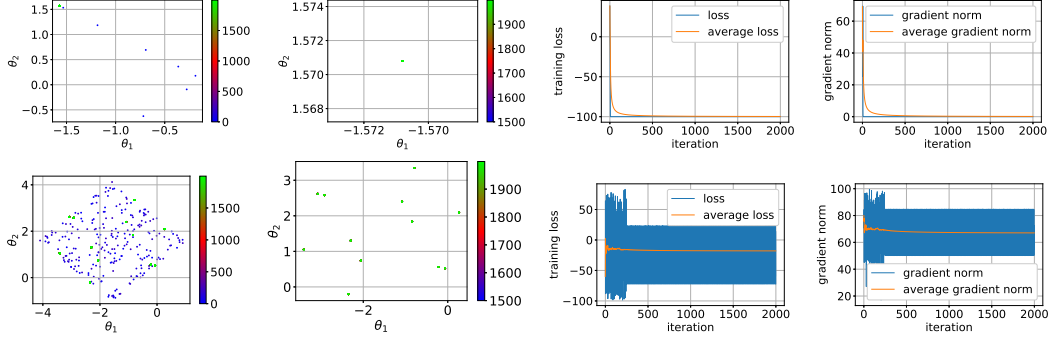


Figure 5: Synthetic experiment. The learning rate is set to be 0.01 and 0.04 for the first and second row respectively. Column I: the whole trajectory in 2000 iterations, where the scatter points correspond to iterates and the color of a point represents which iteration it is at; Column II: the trajectory in the last 500 iterations to show the convergence behavior; Column III: training loss and average training loss vs iteration, where the average is taken over iterations; Column IV: gradient norm and average gradient norm vs iteration.

The second conjecture is refuted by our TransformerXL [Dai et al., 2019a] experiment in Section 2.2. We see that this phenomenon in TransformerXL training is even more eminent.

The third conjecture is refuted by comparing the experiment in Figure 3 against the experiments in the last two row of Figure 2. We see that longer training with larger constant step size also doesn’t solve the problem.

The fourth conjecture is refuted due to our estimation precision discussed in later Section 6.2 with additional experimental details. We also observed that in our Cifar10 experiment in section 6.1, the gradient norm can indeed go to zero.

In the following sections, we attempt to provide a notion of convergence from the theory of dynamical systems. Our proposed explanation is that only the time average of the training loss converges, while the gradient norm is nonzero due to nonsmoothness, and that the actual weight iterates keep oscillating. Before diving into the theorem, we provide a conceptual explanation through a synthetic experiment in the next section.

3 An explanatory experiment

The curious phenomenon discussed above is not limited to neural network training. In what follows we present a simple synthetic example to illustrate the intuition behind the convergence behavior to unstable cycles rather than stationary points.

To this end, we simulate gradient descent on the objective function $f(\theta_1, \theta_2) = 100 \sin \theta_1 \sin \theta_2$ whose smoothness and Lipschitzness parameters are both $L_f = 100$. It is well known that gradient descent with a learning rate $\eta < 2/L_f = 0.02$ provably converges to stationary points for such a smooth function. As shown in the first row of Figure 5, the iterates converge to a fixed point very fast with $\eta = 0.01$, which also implies the convergence of both training loss and gradient norm. Moreover, the gradient norm converges to zero, which means a stationary point is reached at convergence.

However, when $\eta > 2/L_f$, which is often the case for neural network training, gradient descent no longer converges to stationary points as shown in the second row of Figure 5 with $\eta = 0.04$. During the last 500 iterations, the iterates only take values around a few points and keep oscillating among them. As a result, the training loss and gradient norm also oscillate and do not converge in the usual sense. However, the oscillation among these points follows some periodic pattern. If we collect all the iterates during a long enough training process, their empirical distribution will converge to a discrete distribution over those fixed points. As a result, the empirical distributions of the training losses and gradient norms at these iterates also converge. Then if we take an average of the training losses or gradient norms over time, it must converge to the expected value of the corresponding empirical distribution, as shown in the last two images in Figure 5. However, although the

average gradient norm converges, the convergence value can not be zero in presence of oscillation, as gradient descent makes no updates if the gradient is zero.

The above example shows that the key to function value convergence could be that a time average rather than a spatial average is taken in evaluating the function loss. In fact, we could verify this intuition through the example below. Recall that in ImageNet training, the plotted training loss is a moving average of previous iterations. In the left plot of Figure 6 we instead plot the training loss of the last 50 epochs in the experiment shown in Figure 3 and see that the variation across iterations is quite large considering the learning rate is 0.01 and the gradient norm is about 0.6. On the right plot, we show the last a few iterations of transformerXL training (see section 6 for more details) and observe even larger oscillations. Furthermore, even in Cifar10 experiments, both [Li et al. \[2020\]](#), [Lobacheva et al. \[2021\]](#) show very strong periodic divergence in training loss when the number of training epoch is huge (> 1000 epochs).

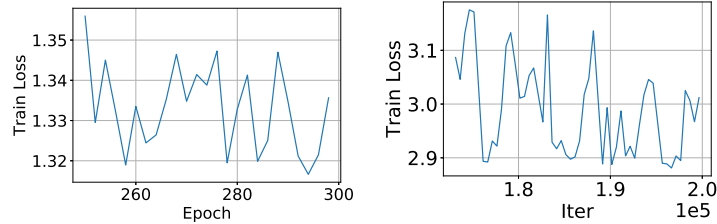


Figure 6: (Left) The training loss vs epochs with a constant learning rate $\eta = 0.01$ in the last 50 epochs of the 300-epoch ImageNet experiment. (Right) The training loss vs epochs with a constant learning rate $\eta = 0.01$ in the last iterations of the 2-million step transformerXL experiment.

Therefore, we see that the loss looks smooth because the oscillation is much smaller than the long-term loss decrease due to optimization. However, the variation is nontrivial considering the step size and gradient norm. Hence, the convergence only happens in the **time average** sense. With this intuition, we are now ready to present a more rigorous characterization of the phenomenon next.

4 Convergence beyond stationary points

We have seen that even though the per-iteration loss does not converge, the time average with a long enough window size can converge. In this section, we provide a simple mathematical analysis to explain why that happens. In particular, we prove that the change in training loss evaluated as a time average converges to 0 for neural networks. Our analysis is motivated by, and closely follows the proof of the celebrated Krylov-Bogolyubov theorem on invariant measures. As a result, we refer to our interpretation as the *invariant measure perspective*.

Our key insight is that the convergence of the training loss occurs in a time-average sense. To see this, consider the following dynamical system

$$\theta_{t+1} = F(\theta_t).$$

The time average naturally leads to the following notion of empirical measure:

$$\mu_k := \frac{1}{k} \sum_{t=1}^k \delta_{\theta_t}, \quad (3)$$

where δ_θ denotes the Dirac measure supported on the value θ , i.e., $\delta_\theta(A) = 1$ if and only if $\theta \in A$, and $\{\theta_1, \theta_2, \dots\}$ are the sequence of iterates generated by the dynamical system.

With this notation, we can conveniently write the time average of a scalar function $\phi : \mathcal{X} \rightarrow \mathbb{R}$ as

$$\mu_k(\phi) = \mathbb{E}_{\theta \sim \mu_k} [\phi(\theta)]. \quad (4)$$

In this work, we focus on the case when the dynamic system $F(\theta_t)$ denotes the SGD update, i.e.,

$$F(\theta_t) = \theta_t - \eta g(\theta_t),$$

where $g(\theta_t)$ denotes the stochastic gradient and η denotes the step size.

4.1 Invariant Measures

We say a measure μ is an **invariant measure** for the map $F : \mathcal{X} \rightarrow \mathcal{X}$ if for any measurable set A

$$\mu(A) = \mu(F^{-1}(A)) = \int_{\theta} \mathbb{1}\{F(\theta) \in A\} d\mu(\theta),$$

where $F^{-1}(A) = \{\theta | F(\theta) \in A\}$. Notice that if F is a stochastic update, then this should be read as

$$\mu(A) = \mu(F^{-1}(A)) = \int_{\theta} \mathbb{P}\{F(\theta) \in A\} d\mu(\theta). \quad (5)$$

Invariance of measure is closely related to convergence of function values when $\theta \sim \mu$ is sampled from an invariant probability measure. In such a scenario, for any continuous function ϕ , the function value does not change after one update,

$$\mathbb{E}_{\theta \sim \mu}[\phi(\theta)] = \mathbb{E}_{\theta \sim \mu}[\phi(F(\theta))].$$

In other words, the function value does not change in expectation. Motivated by this observation, we state the following theorem:

Theorem 1 (convergence of function values). *Consider a continuous scalar function $\phi : \mathcal{X} \rightarrow \mathbb{R}$. Assume that the update map F has the property that $\phi \circ F : \mathcal{X} \rightarrow [-M, M]$ has a bounded value for any $\theta \in \mathcal{X}$, then with probability $1 - \delta$ over the randomness of F ,*

$$|\mathbb{E}_{\theta \sim \mu_n}[\phi(\theta) - \phi(F(\theta))]| = \mathcal{O}\left(\frac{\log(1/\delta)}{\sqrt{n}}\right). \quad (6)$$

Proof. The proof can be found in Appendix A. □

The above theorem shows that for a stochastic dynamical system, any bounded scalar function when evaluated on the empirical measure has vanishing updates as the number of iterations goes to infinity. We will later see how this relates to the vanishing gain of training loss in neural network training.

The tightness of the $1/\sqrt{n}$ dependence in the above theorem easily follows by considering a stochastic map F such that $F(\theta)$ distributes uniformly over \mathcal{X} for any θ . However, the tightness of the dependence on n is less clear when F is deterministic. We show below that even for maps on a compact set, the window size n in the time-average has to tend to infinity for the sequence to converge.

Lemma 2. *For any positive integer n , there exists a 1-Lipschitz objective function f and a positive value $\mathcal{O}(1/n)$ such that the update $F(\theta) = \theta - \nabla f(\theta)$ has a compact invariant set, and the sequence of time average with a window size n starting at iteration t , $M_t = \frac{1}{n} \sum_{i=t}^{t+n-1} f(\theta_i)$ does not converge and*

$$\limsup_{t \rightarrow \infty} |M_t - M_{t-1}| \geq \mathcal{O}(1/n) > 0.$$

Proof. The proof can be found in Appendix B. □

The above result suggests that even for gradient descent update, the per-iteration loss function value $\mathbb{E}_{\theta_t}[\phi(\theta_t)]$ may not converge unless the function value is evaluated as time average $\mu_t(\phi)$. The step size can be chosen arbitrarily but the exact dependence between step size η and window size n and the sequence difference $\limsup_{t \rightarrow \infty} |M_t - M_{t-1}|$ requires further investigation.

We also note the fact that the update vanishes to zero does not imply that the limit $\lim_{t \rightarrow \infty} \mu_t(\phi)$ exists. In fact, an explicit counterexample as stated below.

Theorem 3 (Yoccoz). *There exists a dynamic system with deterministic continuous map $F : \mathcal{X} \rightarrow \mathcal{X}$ on a compact set and a scalar function $\phi \in C^\infty$, such that sequence $\frac{1}{n} \sum_{k \leq n} \phi(\theta_k)$ has no limit, where $\theta_{k+1} = F(\theta_k)$.*

Proof. See the original note in [Yoccoz]. □

Given the above negative result, we provide the following theorem to conclude this section.

Theorem 4 (convergence of distribution). *Assume that F maps a compact set \mathcal{X} to itself. Then the empirical distribution has a subsequence converging weakly to an ergodic distribution. In other words, there exists an invariant distribution μ , and a **subsequence** of positive integers $\{n_k\}_{k \in \mathbb{Z}}$ such that*

$$\mu_{n_k} \rightarrow_w \mu. \quad (7)$$

The proof of the above theorem is similar to the proof for the Krylov-Bogolyubov theorem. We include the proof in Appendix C for completeness. Note that since the iterates may not have a limit, only subsequence convergence is possible. We note that the above two theorems do not make use of the gradient descent structure. Whether the dynamic system resulting from gradient descent has exactly the same property is left as a challenging future problem.

With the above results, we are now ready to prove the vanishing property of the update of training loss in neural network training.

4.2 Vanishing change in training loss of neural networks

We are now ready to provide a theoretical analysis to prove the vanishing gain of training losses in neural network training, and thus explain how the training loss can stabilize even when the norm of the loss function gradient is non-zero. Our analysis is distinct from previous ones in the literature in that it does not assume global Lipschitzness or smoothness, does not rely on bounded noise assumptions, and it does not require perfectly fitting the data as in Neural tangent kernel (NTK) models or mean-field style arguments. The downside of this generality is that we only prove convergence of function values and do not make any comments on local or global optimality or generalization. We believe that remains to be done here and we have just scratched the surface. We will make more comments on this in Section 7.

In order to start the discussion, we define the following L -layer deep neural network $f(x, \theta)$, where x is the input and $\theta = (W_0, \dots, W_{L-1})$ is the network weights:

$$\begin{aligned} x_0 &= x, \\ x_{l+1} &= \sigma_{l+1}(W_l x_l), \quad l = 0, \dots, L-1 \\ f(x, \theta) &= x_L, \end{aligned} \quad (8)$$

where σ_l is a coordinate-wise activation function (e.g., ReLU or sigmoid). In practice, the last layer usually does not use any activation function so σ_L is the identity mapping. We do not consider pooling layers, convolutional layers, or skip connections for now and it should be easy to extend our analysis to these settings. Iteration (8) does not include batch normalization layers which we will analyze later in this section. Given a training dataset $S = \{(x^i, y^i)\}_{i=1}^N$, the empirical training loss is defined as

$$L_S(\theta) := \frac{1}{N} \sum_{i=1}^N \ell(f(x^i, \theta), y^i),$$

where $\ell : \mathbb{R}^d \times [d] \rightarrow \mathbb{R}$ is a loss function and we assume $\|x^i\|_2 \leq 1$. The network is trained by SGD with weight decay, which is equivalent to running SGD on the following regularized loss

$$L_S^\gamma(\theta) := L_S(\theta) + \frac{\gamma}{2} \|\theta\|_2^2,$$

where $\|\theta\|_2$ denotes the ℓ_2 norm of vectorized θ . We will focus on the most widely used loss function for classification tasks, the cross-entropy after softmax, defined as follows.

$$\ell(x, y) = x_y - \log \left(\sum_{j=1}^d e^{x_j} \right), \quad (9)$$

which has the following properties that we will use later.

Lemma 5. *The cross-entropy after softmax loss $\ell : \mathbb{R}^d \times [d] \rightarrow \mathbb{R}$ defined in (9) satisfies*

1. *If $\max_i x_i - \min_i x_i \leq c$, we have $\ell(x, y) \leq c + \log d$ for any $y \in [d]$.*
2. *$\ell(x, y)$ is c_ℓ Lipschitz w.r.t. x for some numerical constant c_ℓ .*

Next, we make the following assumption for the activation function. It holds for most activation functions including ReLU and tanh.

Assumption 1. Each activation function σ_l is (sub)-differentiable and c_σ coordinate-wise Lipschitz for some numerical constant $c_\sigma > 0$. Also assume $\sigma_l(0) = 0$.

Now we can prove the vanishing gain of the function values.

Theorem 6. Suppose θ is initialized within the compact set $C_w := \{(W_0, \dots, W_{L-1}) : \|W_l\|_{op} \leq w\}$ for some $w \leq (\gamma/c_\ell c_\sigma^L)^{1/(L-2)}$. Then the iterate θ_k for every k lies in C_w and the empirical measure generated by SGD with a stepsize $\eta \leq 1/\gamma$ satisfies

$$\mathbb{E}_{\theta \sim \mu_n} [L_S(\theta) - L_S(F(\theta))] = \mathcal{O}(\frac{1}{\sqrt{n}}).$$

We notice that the initialization choice may not always hold in practice, especially when there is batch normalization design. We further note that similar to the above theorem, all (piece-wise) continuous scalar functions including the noise norm are bounded by compactness, and hence should stabilize after long enough training. However, in the third column of Figure 2, the noise norm does not really converge. To explain this observation, we propose the following theorem that studies neural networks with batch normalization.

For simplicity of analysis, we assume the last layer is one of the layers with batch normalization. For a vector x , we use x^2 , $|x|$ and \sqrt{x} to denote its coordinate-wise square, absolute value, and square root respectively. In the l -th layer, if it uses batch normalization, given a batch $\mathcal{B} = \{(x^i, y^i)\}_{i=1}^m$ sampled from some distribution $\mathcal{P}_{\mathcal{B}}$, batch normalization makes the following transformation from $\{x_{l-1}^i\}_{i \in \mathcal{B}}$ to $\{x_l^i\}_{i \in \mathcal{B}}$:

$$\begin{aligned} \mu_{\mathcal{B},l-1} &= \frac{1}{m} \sum_{i \in \mathcal{B}} x_{l-1}^i, \quad \sigma_{\mathcal{B},l-1}^2 = \frac{1}{m} \sum_{i \in \mathcal{B}} (x_{l-1}^i - \mu_{\mathcal{B},l-1})^2, \\ \hat{x}_l^i &= \frac{x_{l-1}^i - \mu_{\mathcal{B},l-1}}{\sqrt{\sigma_{\mathcal{B},l-1}^2 + \epsilon}}, \quad x_l^i = a_l \cdot \hat{x}_l^i + b_l, \end{aligned}$$

where a_l and b_l are the scale and shift parameters to be trained. We also use SGD with weight decay to train the network.

Theorem 7 (With batch normalization). Suppose the parameter of batch normalization layer a_L is initialized within the compact set $|a_L| \leq 2\sqrt{m}/\gamma$. Then the empirical measure generated by SGD with $\eta \leq 1/\gamma$ satisfies

$$\mathbb{E}_{\theta \sim \mu_n, \mathcal{B} \sim \mathcal{P}_{\mathcal{B}}} [L_{\mathcal{B}}(\theta) - L_{\mathcal{B}}(F(\theta))] = \mathcal{O}(\frac{1}{\sqrt{n}}).$$

We have shown in this section how the expected change of the training loss in per iterate update converges to zero for neural network training without any smoothness or Lipschitzness assumptions. One weakness of our analysis is that the limit of the training loss may not exist. However, we are not sure whether or when in real-world experiments this happens, due to some recent research on how the loss could further improve or even diverge in extra long training epochs (> 500 epochs) [Liu et al., 2019, Li et al., 2020, Wightman et al., 2021].

Another caveat is that our gain is measured in terms of empirical measure instead of the last iterate distribution. On the theory side, it is very easy to construct nonconverging last iterate distribution by inducing some periodic loops. On the practice side, we believe that further efforts in understanding last iteration stability are required.

In the next section, by utilizing the structures of stochastic gradient descent, we see some interesting implications if we assume that the iterates are from a distribution when the change in training loss is zero.

5 Implications of the invariant measure theorem

While we have taken the first step, simply showing that the change in training loss converges to zero may not be interesting enough. In particular, up to now, the analysis in the previous section has not

explained when and why the function value could decrease. In this section, we look at implications of the invariant measure perspective from a different angle. We assume that the iterates already come from a distribution where the per step change is zero

$$\mathbb{E}_{\theta \sim \mu_k} [L_S(\theta) - L_S(F(\theta))] = 0,$$

and see what it implies in real world experiments.

5.1 Decreasing stepsize leads to smaller objective values

One well-known observation in neural network training is that when the training loss plateaus, reducing the learning rate can further reduce the objective. This phenomenon can be proved in theory if the function has globally bounded noise and smoothness constant. However, as we showed that the smoothness and noise level changes adversarially to the step size. In this section, we provide a partial explanation on when a smaller step size can decrease the function value. In particular, we consider the neural network setup introduced in Section 4.2. We make the following assumption:

Assumption 2. The neural network is second order differentiable though may not necessarily have bounded smoothness.

Then we could prove that reducing the step size by enough ratio would result in a decrease in function value.

Theorem 8. Consider the stochastic gradient update $F : \mathcal{X} \rightarrow \mathcal{X}$ on a compact set defined as $F(\theta) = \theta - \eta g(\theta)$ for a fixed step size $\eta > 0$. Let μ be the invariant distribution such that $\mathbb{E}_{F, \theta \sim \mu} [L_S(\theta)] = \mathbb{E}_{F, \theta \sim \mu} [L_S(F(\theta))]$. If μ is not supported on stationary points (i.e. $\mathbb{E}_{\theta \sim \mu} [\|\nabla f(\theta)\|_2^2] > 0$), then there exists a small enough $c \in (0, 1)$ such that for any positive step size $\eta' < c\eta$, the update $F'(\theta) = \theta - \eta' g(\theta)$ will lead to a smaller function value, i.e.

$$\mathbb{E}_{F', \theta \sim \mu} [L_S(F'(\theta))] < \mathbb{E}_{\theta \sim \mu} [L_S(\theta)].$$

Proof. See Appendix G. □

The above theorem states that once the change in loss vanishes, by selecting a smaller step size, one could further reduce the loss. This reflects the observation in Figure 1. The challenge in the proof is that reducing the step size might lead to worse smoothness that is too large for the step size, and hence may increase the training objective. To prove the theorem, we draw intuition from the proofs of [Zhang et al., 2020b] and consider the line integral as an expectation. We then apply Markov inequality to control the level of variation caused by nonsmoothness.

5.2 Connections to edge-of-stability and relaxed smoothness

We now provide an informal discussion on how the invariant measure prospective can give insight to the edge-of-stability observation and relaxed smoothness phenomenon. Our argument will be informal and heuristic, and somewhat speculative. We believe a rigorous analysis is both interesting and challenging and leave them as future directions.

We start from the equation in the proof of the previous theorem in Appendix G:

$$\mathbb{E}_{\theta, g} [\|\nabla L_S(\theta)\|_2^2] = \mathbb{E}_{\theta, g} \left[\eta \int_0^1 \int_0^1 \langle \nabla L_S(\theta) - g(\theta), \nabla^2 L_S(\gamma_{\theta, g}(t\tau\eta))g(\theta) \rangle dt d\tau \right]$$

where $g(\theta)$ is the stochastic gradient and $\gamma_{\theta, g(\theta)}(r) = \theta - rg(\theta)$ denotes the line segment. Clearly, both sides are positive. We boldly extract an equation

$$\text{Grad}^2 = \eta \Sigma \mathcal{L} G, \tag{10}$$

where Grad denotes the gradient norm, Σ denotes the noise norm, \mathcal{L} denotes the sharpness and G denotes the square root of the second moment of stochastic gradients. This is of course very rough, and is only true when we replace the inner product on the right hand side with its Cauchy-Schwartz upper bound, yet it has some interesting connection to the following two observations.

First, we recall the edge-of-stability framework [Cohen et al., 2021], which observes that the actual smoothness constant during training neural network has an inverse relation to step size. This is true from the above equation if we hold $\text{Grad}, \eta, \Sigma, G$ constant.

Second, in another work [Zhang et al., 2019], the authors identified a positive correlation between the gradient norm and the smoothness constant. This relation can also be extracted from the equation if all other quantities are held constant.

In fact, as we observe that in practice, the relation between the sharpness and step size is not a direct inverse but indeed has some negative correlation. Therefore, we believe by studying the property of the equilibrium, one could understand why many anti-intuition behaviors could happen.

6 Additional experiments details

In this section, we add some additional experiments and experimental details that supplement the results in Section 2. We showed that the observed phenomenon happens in large scale tasks. To supplement the result, we briefly comment on how smaller dataset presents different behavior by taking Cifar experiment as an example. In the end, we will discuss some experimental details on how the quantities in (2) are estimated.

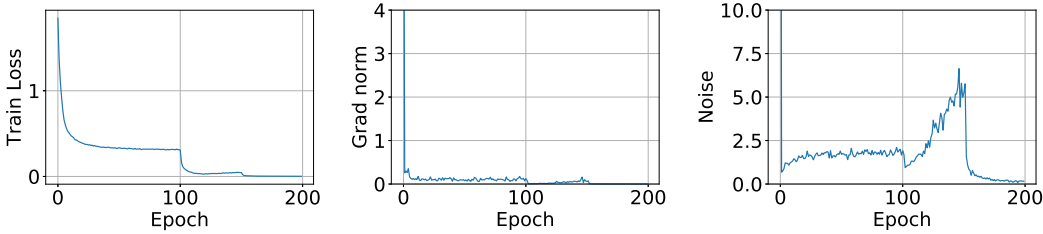


Figure 7: The estimated stats vs epoch for Cifar10 training. The learning rate starts at 0.1 and decay by a factor of 10 at epoch 100 and epoch 150.

6.1 Cifar10 Experiment

In this section, we show how noise, gradient norm and training loss evolve in Cifar10 with ResNet training. Our training procedure is based on the implementation². The key result is demonstrated in Figure 7. We observe that in this case, the gradient norm indeed converges to 0. In fact, this is expected, as for cross entropy loss, the train loss could bound the gradient norm when weights are bounded.

The implications of the above observations are many. First, this separation behavior between small overfitting model on Cifar10 and larger model on ImageNet shows that the study of overparametrization and convergence to stationary point may still be true in many cases. However, we should be careful that these analysis does not apply to larger models that do not overfit the data. Second, this shows that the SDE modeling in [Li et al., 2020, Lobacheva et al., 2021] can also be valid. It also shows that our work studies a problem of a different nature (non-zero grad norm).

6.2 Estimating the statistics

Here we provide additional details on how the values in (2) are estimated. Notice that these quantities are defined using all N data points in the entire dataset, which is too large in practice. Therefore, we use a random batch $m < N$ to estimate the quantities. For training loss, gradient norm, and noise norm, the estimation is straight-forward. For the sharpness, we follow the implementation in [Wu et al., 2018]³ and estimate the sharpness via power iterations.

By Jensen’s inequality, the estimated norms would be larger than the true value. However, the value should converge as the sampled batch size m converges to the total data number N . We show in Figure 8 and Figure 9 how these estimator values converge in practice. Based on these plots, we select the batch size to be 1.6×10^5 for ImageNet training and the token size to be 9×10^5 for the WT103 training. These sample sizes give a high enough precision level for making the observations

²<https://github.com/kuangliu/pytorch-cifar>

³<https://github.com/leiwu0/sgd.stability>

in previous sections. Note that the estimated smoothness for the ImageNet experiment has very large variations, and hence we didn't make many comments on that plot throughout this work.

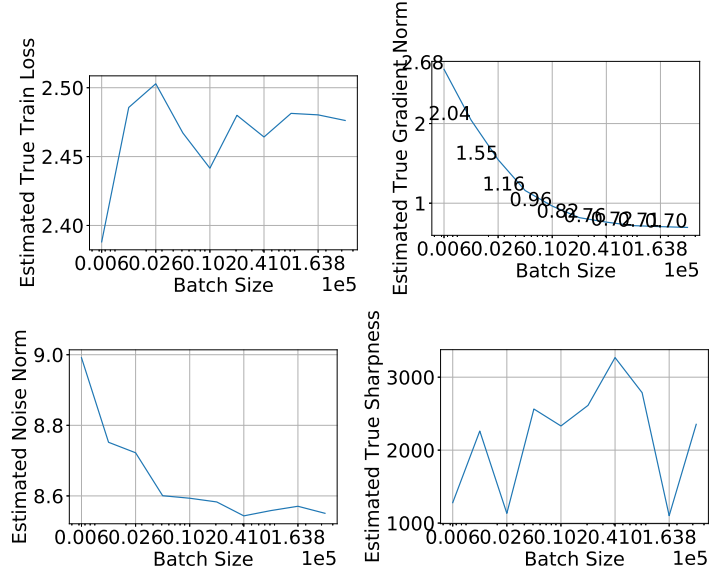


Figure 8: The estimated stats vs batch size for ImageNet training.

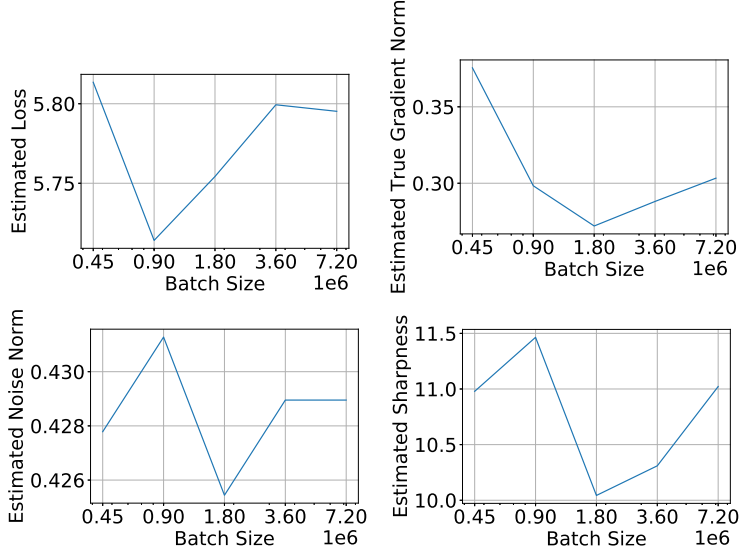


Figure 9: The estimated stats vs batch size for WT103 training.

7 Conclusions and discussions

We identified a key gap between optimization theory and deep learning practice, namely, that during training with (stochastic) gradient descent, weights do not converge to stationary points of the loss function. Our numerical experiments reveal that this phenomenon cannot be eliminated by using a smaller learning rate or more training epochs. We further show that this is prevalent in applications from image classification to language modeling tasks. Using dynamical systems theory, we show that the convergence of training loss is only in the time average sense and that per iteration oscillation, though small compared to the long term trend, is significant compared to the step size, confirming the oscillation of iterates.

Our work provides a paradigm shift in how convergence of weights and loss function should be analyzed and defined *when iterates fail to converge to a single point and distribution of weights do not converge to a globally unique stationary distribution*. We believe that answering this question would require vastly different analysis techniques compared to standard optimization theory. We believe that this paradigm shift may lead to theoretical results with greater empirical impacts.

We took the first step in providing an invariant measure perspective according to which instead of analyzing a single trajectory of weights during training we study whether distribution of values that the weights take under the action of the gradient-based algorithms converge to an invariant measure. More specifically, we showed that the empirical measure has a subsequence that converges to an invariant measure and provide a negative example from [Yoccoz] that shows the sequence of distributions itself may not converge. An open question we left unanswered is whether the sequence itself can converge when the dynamical system follows a fixed step size update. A more interesting question for this research is to characterize the invariant measure and the conditions under which it may be unique, as well as to study convergence rate by exploiting more of the structure from neural network and gradient updates.

Our result only proves that for multilayer perceptron, the weights under the action of the gradient update stay within a compact invariant set. Yet, we did not analyze the dependence of function properties (such as smoothness) on the initialization and optimizer hyperparameters. Understanding the dependence may naturally lead to better understanding and better algorithms. Another interesting question for future research would be to investigate the properties of the invariant measure and training loss as a function of the stepsize.

8 Acknowledgement

This work is supported by NSF CAREER grant (1846088), ONR N00014-20-12394, IIS young scholar fellowship and an MIT-IBM Watson grant.

References

- Y. Arjevani, Y. Carmon, J. C. Duchi, D. J. Foster, N. Srebro, and B. Woodworth. Lower bounds for non-convex stochastic optimization. *arXiv preprint arXiv:1912.02365*, 2019.
- S. Bhojanapalli, K. Wilber, A. Veit, A. S. Rawat, S. Kim, A. Menon, and S. Kumar. On the reproducibility of neural network predictions. Feb. 2021.
- Y. Carmon, J. C. Duchi, O. Hinder, and A. Sidford. Lower bounds for finding stationary points i. *arXiv preprint arXiv:1710.11606*, 2017.
- X. Cheng, D. Yin, P. Bartlett, and M. Jordan. Stochastic gradient and langevin processes. In *International Conference on Machine Learning*, pages 1810–1819. PMLR, 2020.
- Y. K. Cheung and G. Piliouras. Vortices instead of equilibria in minmax optimization: Chaos and butterfly effects of online learning in zero-sum games. In *Conference on Learning Theory*, pages 807–834. PMLR, 2019.
- J. M. Cohen, S. Kaur, Y. Li, J. Z. Kolter, and A. Talwalkar. Gradient descent on neural networks typically occurs at the edge of stability. Feb. 2021.
- Z. Dai, Z. Yang, Y. Yang, J. Carbonell, Q. V. Le, and R. Salakhutdinov. Transformer-xl: Attentive language models beyond a fixed-length context. *arXiv preprint arXiv:1901.02860*, 2019a.
- Z. Dai, Z. Yang, Y. Yang, J. G. Carbonell, Q. V. Le, and R. Salakhutdinov. Transformer-XL: Attentive language models beyond a fixed-length context. *CoRR*, abs/1901.02860, 2019b. URL <http://arxiv.org/abs/1901.02860>.
- A. Defazio and L. Bottou. On the ineffectiveness of variance reduced optimization for deep learning. *arXiv preprint arXiv:1812.04529*, 2018.
- C. Fang, C. J. Li, Z. Lin, and T. Zhang. Spider: Near-optimal non-convex optimization via stochastic path integrated differential estimator, 2018.

L. Flokas, E.-V. Vlatakis-Gkaragkounis, T. Lianeas, P. Mertikopoulos, and G. Piliouras. No-regret learning and mixed nash equilibria: They do not mix. *arXiv preprint arXiv:2010.09514*, 2020.

M. Gurbuzbalaban, U. Simsekli, and L. Zhu. The heavy-tail phenomenon in sgd. In *International Conference on Machine Learning*, pages 3964–3975. PMLR, 2021.

K. He, X. Zhang, S. Ren, and J. Sun. Deep residual learning for image recognition. In *Proceedings of the IEEE conference on computer vision and pattern recognition*, pages 770–778, 2016.

P. Henderson, R. Islam, P. Bachman, J. Pineau, D. Precup, and D. Meger. Deep reinforcement learning that matters. Sept. 2017.

Y.-G. Hsieh, F. Iutzeler, J. Malick, and P. Mertikopoulos. On the convergence of single-call stochastic extra-gradient methods. *arXiv preprint arXiv:1908.08465*, 2019.

D. P. Kingma and J. Ba. ADAM: A method for stochastic optimization. *arXiv preprint arXiv:1412.6980*, 2014.

D. Kunin, J. Sagastuy-Brena, L. Gillespie, E. Margalit, H. Tanaka, S. Ganguli, and D. L. Yamins. Rethinking the limiting dynamics of sgd: modified loss, phase space oscillations, and anomalous diffusion. *arXiv preprint arXiv:2107.09133*, 2021.

A. Letcher. On the impossibility of global convergence in multi-loss optimization. *arXiv preprint arXiv:2005.12649*, 2020.

Z. Li, K. Lyu, and S. Arora. Reconciling modern deep learning with traditional optimization analyses: The intrinsic learning rate. *Advances in Neural Information Processing Systems*, 33, 2020.

Y. Liu, M. Ott, N. Goyal, J. Du, M. Joshi, D. Chen, O. Levy, M. Lewis, L. Zettlemoyer, and V. Stoyanov. Roberta: A robustly optimized bert pretraining approach. *arXiv preprint arXiv:1907.11692*, 2019.

E. Lobacheva, M. Kodryan, N. Chirkova, A. Malinin, and D. Vetrov. On the periodic behavior of neural network training with batch normalization and weight decay. *arXiv preprint arXiv:2106.15739*, 2021.

P. Madhyastha and R. Jain. On model stability as a function of random seed. Sept. 2019.

C. Papadimitriou and G. Piliouras. Game dynamics as the meaning of a game. *ACM SIGecom Exchanges*, 16(2):53–63, 2019.

S. J. Reddi, S. Kale, and S. Kumar. On the convergence of ADAM and beyond. *arXiv preprint arXiv:1904.09237*, 2019.

R. Wightman, H. Touvron, and H. Jégou. Resnet strikes back: An improved training procedure in timm, 2021.

L. Wu, C. Ma, et al. How sgd selects the global minima in over-parameterized learning: A dynamical stability perspective. *Advances in Neural Information Processing Systems*, 31:8279–8288, 2018.

J.-C. Yoccoz. An example of non convergence of birkhoff sums. https://www.college-de-france.fr/media/jean-christophe-yoccoz/UPL54030_birkhoff.pdf.

J. Zhang, T. He, S. Sra, and A. Jadbabaie. Why gradient clipping accelerates training: A theoretical justification for adaptivity. May 2019.

J. Zhang, H. Lin, S. Das, S. Sra, and A. Jadbabaie. Stochastic optimization with non-stationary noise. *arXiv preprint arXiv:2006.04429*, 2020a.

J. Zhang, H. Lin, S. Jegelka, A. Jadbabaie, and S. Sra. Complexity of finding stationary points of nonsmooth nonconvex functions. Feb. 2020b.

A Proof of Theorem 1

Proof. By the fact that $\phi \circ F : \mathcal{X} \rightarrow \mathbb{R}$ has bounded value $[-M, M]$, we can denote the subgaussian norm at θ as

$$\sigma(\theta) = \inf\{\sigma > 0 | \mathbb{P}(\|\phi(F(\theta)) - \mathbb{E}[\phi(F(\theta))]\| \geq t) \leq 2e^{-t^2/2\sigma^2}\}.$$

In fact, $\forall \theta, \sigma(\theta) \leq M < \infty$. Hence, we can further denote the upperbound on the sub-Gaussian norm as

$$\sigma = \sup_{\theta} \sigma(\theta).$$

Then we consider two distributions. One is the empirical distribution of a sampled trajectory,

$$\mu_n = \frac{1}{n} \sum_{t=1}^n \delta_{\theta_t}.$$

The other one is the pushforward distribution $\mu_k(F^{-1})$ as defined in (5). Then,

$$\begin{aligned} \mathbb{E}_{\theta \sim \mu_n} [\phi(\theta) - \phi(F(\theta))] &= \frac{1}{n} \sum_{t=1}^n \phi(\theta_t) - \frac{1}{n} \sum_{t=1}^n \phi(F(\theta_t)) \\ &= \frac{1}{n} (\phi(\theta_0) - \phi(F(\theta^n))) + \frac{1}{n} \sum_{t=1}^n \phi(\theta_t) - \phi(F(\theta_{-1})) \\ &= \mathcal{O}\left(\frac{1}{n}\right) + \frac{1}{n} \sum_{t=1}^n \phi(\theta_t) - \phi(F(\theta_{t-1})). \end{aligned}$$

Then the claim follows by applying Hoeffding's inequality on the second term. \square

B Proof of Lemma 2

Proof. First, we construct a function

$$f(\theta) = \begin{cases} -\frac{1}{n+1}\theta & \theta \leq 0, \\ \frac{n}{n+1}\theta & \theta > 0. \end{cases} \quad (11)$$

We notice that if $\theta_0 = \frac{0.2}{n+1}$, then $\theta_k = -1 + \frac{k-0.8}{n+1}$, $k \leq n$ and $\theta_0, \theta_1, \theta_2, \dots, \theta_n$ is periodic with period $n+1$. We further notice that within a period $\theta_1, \dots, \theta_{n+1}$, the function values are distinct, and $|f(\theta_0) - f(\theta_1)| \geq 0.5$. Therefore, for any $n > 0$, there exists a $t > n$ such that

$$|M_t - M_{t-1}| = \frac{1}{n} |f(\theta_{t+n-1}) - f(\theta_{t-1})| \geq \frac{1}{2n}.$$

\square

C Proof of Theorem 4

Proof. Since \mathcal{X} is a compact metric space, we can find a dense countable set of the family of continuous functions $C(\mathcal{X})$, denoted as $\{\phi_1, \phi_2, \dots\}$. Since \mathcal{X} is compact, we have that $\mu_k(\phi_j)$ exists for any k, j . Therefore, by the diagonal argument, there exists a subsequence $\{n_k\}_k$ such that for all $j = 1, 2, \dots$,

$$\lim_{k \rightarrow \infty} \frac{1}{n_k} \sum_{l \leq n_k} \phi_j(\theta_l) = J(\phi_j).$$

Then by denseness of the set $\{\phi_1, \phi_2, \dots\}$, we know that the above limit also exists for any $\phi \in C(\mathcal{X})$. Denote the functional as

$$J(\phi) = \lim_{k \rightarrow \infty} \frac{1}{n_k} \sum_{l \leq n_k} \phi(\theta_l). \quad (12)$$

Since J is obviously linear and bounded, there exist a unique probability measure ϕ such that $J(\phi) = \mu(\phi)$.

The invariance of μ follows by the fact that for any continuous ϕ ,

$$\begin{aligned}
\lim_{k \rightarrow \infty} |\mathbb{E}_{\theta \sim \mu_k} [\phi(\theta) - \phi(F(\theta))]| &= \lim_{k \rightarrow \infty} \frac{1}{n_k} \sum_{l \leq n_k} \phi(\theta_l) - \frac{1}{n_k} \sum_{l \leq n_k} \phi(F(\theta_l)) \\
&= \lim_{k \rightarrow \infty} \frac{1}{n_k} \sum_{l \leq n_k} \phi(\theta_l) - \frac{1}{n_k} \sum_{l \leq n_k} \phi(\theta_{l+1}) \\
&\quad + \lim_{k \rightarrow \infty} \frac{1}{n_k} \sum_{l \leq n_k} \phi(\theta_{l+1}) - \frac{1}{n_k} \sum_{l \leq n_k} \phi(F(\theta_l)) \\
&= \lim_{k \rightarrow \infty} \frac{1}{n_k} (\phi(\theta_1) - \phi(\theta_{n_k+1})) \\
&\quad + \lim_{k \rightarrow \infty} \frac{1}{n_k} \sum_{l \leq n_k} (\phi(\theta_{l+1}) - \phi(F(\theta_l))) \rightarrow 0. \quad (13)
\end{aligned}$$

In the last line, the first term goes to zero by boundedness of function value on the compact set. The second term goes to zero by noticing that the sequence

$$M_n = \frac{1}{n} \sum_{l \leq n} (\phi(\theta_{l+1}) - \phi(F(\theta_l)))$$

is a martingale sequence. By the fact that each the induced martingale difference sequence has uniformly bounded sub-Gaussian norm, we can apply Hoeffding's inequality and know that M_n converge in probability to 0, which implies convergence in distribution.

□

D Proof of Lemma 5

Proof.

1. Let $x_m = (\max_i x_i + \min_i x_i)/2$ and define $z_i = x_i - x_m$. We know $|z_i| \leq c/2$. Then we have

$$\begin{aligned}
|\ell(x, y)| &= \left| z_y + x_m - \log \left(\sum_{j=1}^d e^{z_j + x_m} \right) \right| \\
&= \left| z_y - \log \left(\sum_{j=1}^d e^{z_j} \right) \right| \\
&\leq c/2 + \log \left(d e^{c/2} \right) \\
&= c + \log d.
\end{aligned}$$

2. As ℓ is differentiable, it suffices to bound its gradient norm. For any fixed $1 \leq k \leq d$, we have

$$\frac{\partial \ell(x, y)}{\partial x_k} = \delta_{y,k} - \frac{e^{x_k}}{\sum_{j=1}^d e^{x_j}}.$$

Then we can bound

$$\begin{aligned}
\left\| \frac{\partial \ell(x, y)}{\partial x} \right\|_2 &= \sqrt{\sum_{k=1}^d \left(\frac{\partial \ell(x, y)}{\partial x_k} \right)^2} \\
&\leq \sqrt{1 + \frac{\sum_{k=1}^d e^{2x_k}}{\left(\sum_{j=1}^d e^{x_j} \right)^2}} \\
&\leq \sqrt{2}.
\end{aligned}$$

□

E Proof of Theorem 6

Proof. Denote $\rho = wc_\sigma$. Then it is easy to show that within C_w , we have $\|x_l\|_2 \leq \rho^l$ for every l . We define $z_{l+1} = W_l \theta_l$ and thus $x_l = \sigma_l(z_l)$. For any mini-batch $\mathcal{B} = \{(x^i, y^i)\}_{i=1}^m$, we can bound the gradient norm of the loss.

$$\left| \frac{\partial L_{\mathcal{B}}}{\partial W_l} \right| = \left| \frac{1}{m} \sum_{i \in \mathcal{B}} x_l^i (\nabla_x \ell(x_L^i, y^i))^\top D_L^{(i)} \left(\prod_{s=l+1}^{L-1} W_s D_s^{(i)} \right) \right| \leq c_\ell c_\sigma \rho^{L-1} \leq \gamma w,$$

where we define $D_l^{(i)} = \text{Diag}(\sigma'_l(z_l^i))$. By the SGD rule, we have

$$W_l^{k+1} = (1 - \eta\gamma)W_l^k - \eta \frac{\partial L_{\mathcal{B}}}{\partial W_l}.$$

Choosing $\eta \leq 1/\gamma$, if $\|W_l^k\|_{\text{op}} \leq w$, we also have

$$\|W_l^{k+1}\|_{\text{op}} \leq (1 - \eta\gamma)w + \eta\gamma w \leq w.$$

By induction on k , the iterates of SGD optimizing the above objective always lie in C_w if the stepsize satisfies $\eta \leq 1/\gamma$. Then we have $\|x_L^i\|_2 \leq \rho^L$ and can bound that for any k

$$|L_{\mathcal{B}}(\theta_k)| \leq \log d + c_\ell \|x_L^i\|_2 \leq \log d + \left(\frac{\gamma}{c_\ell c_\sigma^2} \right)^{L/(L-2)}.$$

The claim then follows by applying Theorem 1. \square

F Proof of Theorem 7

Proof. We first show that the coordinates of \hat{x}_L^i are bounded.

$$|\hat{x}_L^i| = \frac{|x_{L-1}^i - \mu_{\mathcal{B}, L-1}|}{\sqrt{\frac{1}{m} \sum_{i \in \mathcal{B}} (x_{L-1}^i - \mu_{\mathcal{B}, L-1})^2 + \epsilon}} \leq \sqrt{m}.$$

As in Theorem 6, we show that during the training process, a_L always satisfies $|a_L| \leq 2\sqrt{m}/\gamma$. Note that

$$\begin{aligned} \left| \frac{\partial L_{\mathcal{B}}}{\partial a_L} \right| &= \left| \frac{1}{m} \sum_{i \in \mathcal{B}} \hat{x}_L^i \cdot \nabla_x \ell(x_L^i, y^i) \right| \\ &= \left| \frac{1}{m} \sum_{i \in \mathcal{B}} \sum_{k=1}^d (\hat{x}_L^i)_k \left(\delta_{y,k} - \frac{e^{(x_L^i)_k}}{\sum_{j=1}^d e^{(x_L^i)_j}} \right) \right| \\ &\leq \max_{i \in \mathcal{B}} \left| (\hat{x}_L^i)_y - \frac{\sum_{k=1}^d (\hat{x}_L^i)_k e^{(x_L^i)_k}}{\sum_{j=1}^d e^{(x_L^i)_j}} \right| \\ &\leq 2\sqrt{m}. \end{aligned}$$

Therefore if $|a_L^k| \leq 2\sqrt{m}/\gamma$, we have

$$|a_L^{k+1}| = \left| (1 - \eta\gamma) a_L^k - \eta \frac{\partial L_{\mathcal{B}}}{\partial a_L} \right| \leq (1 - \eta\gamma) \cdot 2\sqrt{m}/\gamma + 2\eta\sqrt{m} \leq 2\sqrt{m}/\gamma.$$

Then by induction, the above is true for every k . By Lemma 5, we have for every k

$$L_{\mathcal{B}}(\theta_k) \leq 4m/\gamma + \log d.$$

Then the training loss $|L_{\mathcal{B}}(\theta_k)| \leq 4m/\gamma + \log d$ is bounded during the training process if the stepsize satisfies $\eta \leq 1/\gamma$. The theorem follows by applying Theorem 1. \square

G Proof of Theorem 8

Proof. For simplicity, we denote

$$\begin{aligned} f(\theta) &:= L_S(\theta), \\ \delta &:= \mathbb{E}_{\theta \sim \mu}[\|\nabla f(\theta)\|_2^2] > 0. \end{aligned}$$

By compactness of \mathcal{X} , we could denote the following quantities:

$$\begin{aligned} G &= \sup_{\theta \in \mathcal{X}} \|g(\theta)\|_2 < \infty, \\ M^2 &= \sup_{\theta, \zeta \in \mathcal{X}} \mathbb{E}_{z \sim \text{unif}[\theta, \zeta]}[\|\nabla^2 f(z) - \mathbb{E}_{z' \sim \text{unif}[\theta, \zeta]}[\nabla^2 f(z')]\|_{\text{op}}^2] < \infty, \\ \Sigma &= \sup_{\theta \in \mathcal{X}} \|g(\theta) - \nabla f(\theta)\|_2 < \infty. \end{aligned}$$

For clarity, note that for any function $f : \mathcal{X} \rightarrow \mathbb{R}^d$,

$$\mathbb{E}_{z \sim \text{unif}[\theta, \zeta]}[f(z)] = \int_0^1 f(t\theta + (1-t)\zeta) dt.$$

Therefore, we have that for any $c \in (0, 1)$

$$\begin{aligned} &\int_0^1 \|\nabla^2 f(ct\theta + (1-ct)\zeta) - \mathbb{E}_{z \sim \text{unif}[\theta, \zeta]}[\nabla^2 f(z)]\|_{\text{op}}^2 dt \\ &= \frac{1}{c} \int_0^c \|\nabla^2 f(t\theta + (1-t)\zeta) - \mathbb{E}_{z \sim \text{unif}[\theta, \zeta]}[\nabla^2 f(z)]\|_{\text{op}}^2 dt \\ &\leq \frac{1}{c} \mathbb{E}_{z \sim \text{unif}[\theta, \zeta]}[\|\nabla^2 f(z) - \mathbb{E}_{z' \sim \text{unif}[\theta, \zeta]}[\nabla^2 f(z')]\|_{\text{op}}^2]. \end{aligned}$$

Therefore, by Jensen's inequality, we have

$$\int_0^1 \|\nabla^2 f(ct\theta + (1-ct)\zeta) - \mathbb{E}_{z \sim \text{unif}[\theta, \zeta]}[\nabla^2 f(z)]\|_{\text{op}} dt \leq \sqrt{\frac{M^2}{c}}. \quad (14)$$

By applying Taylor expansion twice we get the following equations,

$$\begin{aligned} \mathbb{E}_{\theta, F}[f(\theta) - f(F(\theta))] &= \mathbb{E}_{\theta, g}[f(\theta) - f(\theta - \eta g(\theta))] \\ &= \mathbb{E}_{\theta, g}[-\eta \int_0^1 \langle g(\theta), \nabla f(\gamma_{\theta, g(\theta)}(\eta t)) \rangle dt] \\ &= \mathbb{E}_{\theta, g}[-\eta \|\nabla f(\theta)\|_2^2 + \eta \int_0^1 \langle g(\theta) - \nabla f(\theta), \nabla f(\gamma_{\theta, g(\theta)}(\eta t)) \rangle dt] \\ &= \mathbb{E}_{\theta, g}[-\eta \|\nabla f(\theta)\|_2^2 + \eta \int_0^1 \langle g(\theta) - \nabla f(\theta), \nabla f(\gamma_{\theta, g(\theta)}(\eta t)) - \nabla f(\theta) \rangle dt] \\ &= \mathbb{E}_{\theta, g}[-\eta \|\nabla f(\theta)\|_2^2 - \eta^2 \int_0^1 \int_0^1 \langle g(\theta) - \nabla f(\theta), \nabla^2 f(\gamma_{\theta, g(\theta)}(t\tau\eta)) g(\theta) \rangle dt d\tau]. \end{aligned}$$

where $\gamma_{\theta, g(\theta)}(r) = \theta - rg(\theta)$ denotes the line segment.

By invariance of the function value, we get that

$$\begin{aligned} &\mathbb{E}_{\theta, g}[-\eta \|\nabla f(\theta)\|_2^2 - \eta^2 \int_0^1 \int_0^1 \langle g(\theta) - \nabla f(\theta), \nabla^2 f(\gamma_{\theta, g(\theta)}(t\tau\eta)) g(\theta) \rangle dt d\tau] = 0 \\ \implies &\mathbb{E}_{\theta, g}[\|\nabla f(\theta)\|_2^2] = \mathbb{E}_{\theta, g}[\eta \int_0^1 \int_0^1 \langle \nabla f(\theta) - g(\theta), \nabla^2 f(\gamma_{\theta, g(\theta)}(t\tau\eta)) g(\theta) \rangle dt d\tau]. \end{aligned}$$

Therefore we have that

$$\begin{aligned}
& \mathbb{E}_{\theta, F'}[f(\theta) - f(F'(\theta))] \\
&= \mathbb{E}_{\theta, g}[-c\eta \|\nabla f(\theta)\|_2^2 - c^2\eta^2 \int_0^1 \int_0^1 \langle g(\theta) - \nabla f(\theta), \nabla^2 f(\gamma_{\theta, g}(t\tau\eta))g(\theta) \rangle dt d\tau] \\
&\leq c\eta \left(-\delta + c\Sigma G \sqrt{\frac{M}{c}} \right),
\end{aligned}$$

where in the last line we used (14). The claim follows by setting c small enough. \square